Communication

Extending the Capability of STM Break Junction for Conductance Measurement of Atomic-Size Nanowires: An Electrochemical Strategy

Xiao-Shun Zhou, Yi-Min Wei, Ling Liu, Zhao-Bin Chen, Jing Tang, and Bing-Wei Mao

J. Am. Chem. Soc., **2008**, 130 (40), 13228-13230 • DOI: 10.1021/ja8055276 • Publication Date (Web): 13 September 2008

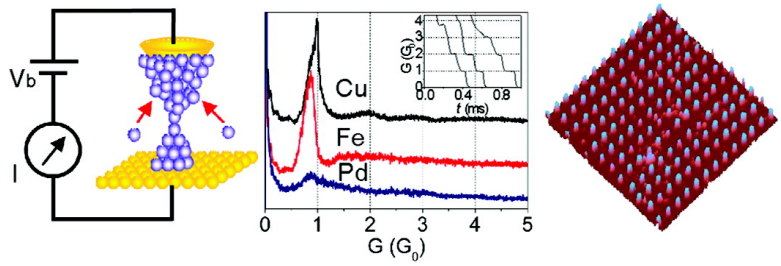

More About This Article

Additional resources and features associated with this article are available within the HTML version:

- Supporting Information
- Access to high resolution figures
- Links to articles and content related to this article
- Copyright permission to reproduce figures and/or text from this article

View the Full Text HTML

J|A|C|S
COMMUNICATIONS

Published on Web 09/13/2008

Extending the Capability of STM Break Junction for Conductance Measurement of Atomic-Size Nanowires: An Electrochemical Strategy

Xiao-Shun Zhou, Yi-Min Wei, Ling Liu, Zhao-Bin Chen, Jing Tang, and Bing-Wei Mao*

State Key Laboratory of Physical Chemistry of Solid Surfaces and Department of Chemistry, College of Chemistry and Chemical Engineering, Xiamen University, Xiamen 361005, China

Received July 25, 2008; E-mail: bwmao@xmu.edu.cn

The STM break junction (STM-BJ) and mechanically controllable break junction (MCBJ) are the two most widely applied techniques to fabricate atomic-size nanowires for quantum conductance measurements.[1−8] In both techniques, a metallic contact is created by approaching a pair of counterfacing metal electrodes made of the same materials, which is followed by stretching the contact to form an atomic-size constriction with decreasing diameter. The conductance of a variety of metals, including noble metal, transition metal, and alkali metal,[1] has been investigated at low temperature[5−8] and/or room temperature[2−4,9] as well as in vacuum,[4−8] ambient,[9] and even electrochemical environments.[2,3] These studies have led to significant advances in understanding the point-contact conductance of metals and their dependence on the properties of the valence electron orbital.

However, the conventional STM-BJ and MCBJ techniques suffer from several drawbacks of the mechanical crashing of the two electrodes of the same materials, which limit the capability in view of the variety of metals as well as the environment to perform the measurement. (i) For some metals such as Pd and Fe, it is hard to create a chemically well-defined atomic-size contact through mechanical crashing of the two electrodes of the same materials, and conduction properties of these metals are still unclear. (ii) For chemically active metals, direct employment of them as the tip and substrate appears tough, if not impossible, in an electrochemical environment. (iii) The above-mentioned drawbacks potentially restrict the variety of metal-molecule-metal junctions, which is important for systematic studies of single molecule conductance beyond the Au-molecule-Au junctions that has presently been dominating in the field.[10−17]

Continuous efforts have been devoted to construct the metallic atomic-size nanowires for conductance measurement by electrochemical means.[2,3,18−21] Tao and co-workers[18,19] and later Murakoshi and co-workers[20] demonstrated the conductance measurements by controlled deposition and dissolution of metals, which allows natural formation and breaking of the metallic nanowires. Such an approach, however, has the weakness in performing a statistically large number of measurements required to construct conductance histograms. More recently, Murakoshi and co-workers deposited metals onto both the tip and substrate of the STM, which is then followed by repetitive STM-BJ measurements.[3,21] However, since the tip and substrate are deposited with the same material, most of the problems encountered in the conventional STM-BJ technique mentioned above remain unsolved.

In this communication, we present an electrochemical strategy to extend the capability of STM-BJ to create nanowires of various metals. The principle of the approach is based on the electrochemical STM tip-induced nanostructuring[22−26] and is illustrated in Figure 1. The tip and substrate are made of the same metal (M_1). A metal of interest (M_2), which is dissimilar to yet unlikely to form a severe surface alloy at room temperature with M_1 is being

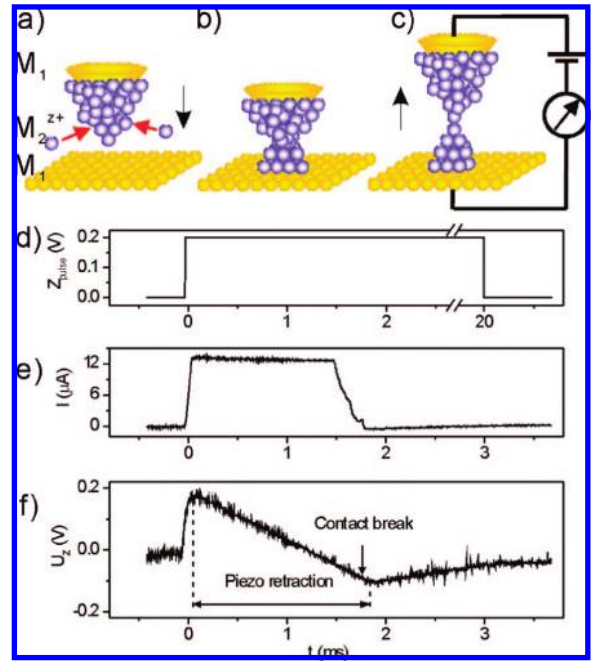

Figure 1. Schematic illustration of the electrochemically assisted and jump-to-contact facilitated strategy for STM-BJ (a−c) and the actual tip current and z-piezo voltage response recorded by an oscilloscope upon application of an external voltage pulse (d−f).

continuously electrodeposited onto the tip (Figure 1a). A short voltage pulse (Z_{pulse}, Figure 1d) is superimposed onto the z-piezo voltage of the STM operated in a constant-current mode. With proper settings of proportional and integral gains, the tip is driven toward the surface to a sufficiently close distance within a short period of time (<1 ms) so that a jump-to-contact occurs. Usually, atoms of M_2 on the tip transfer to the surface to create a nanoconstriction of M_2, Figure 1b. The STM feedback circuit automatically responds to the sharp rise of the current upon contact (Figure 1e) by retracting the piezo with a linear decrease of the voltage at the piezo (U_z, Figure 1f). Hence, the nanoconstriction is gradually stretched to atomic size and eventually breaks, during which the current trace is recorded simultaneously. By repeating the whole process always at new positions of the surface to ensure the well-controlled jump-to-contact mechanism, thousands of current traces can be recorded, from which conductance histogram can be constructed. Such an electrochemically assisted and jump-to-contact facilitated strategy would extend the capability of STM-BJ to form a chemically well-defined contact, based on which variety of atomic-size nanowires of the deposited metals can be formed for conductance measurement.

The feasibility of the present approach is first demonstrated by taking Cu as a model system. The conductance measurements were

10.1021/ja8055276 CCC: $40.75

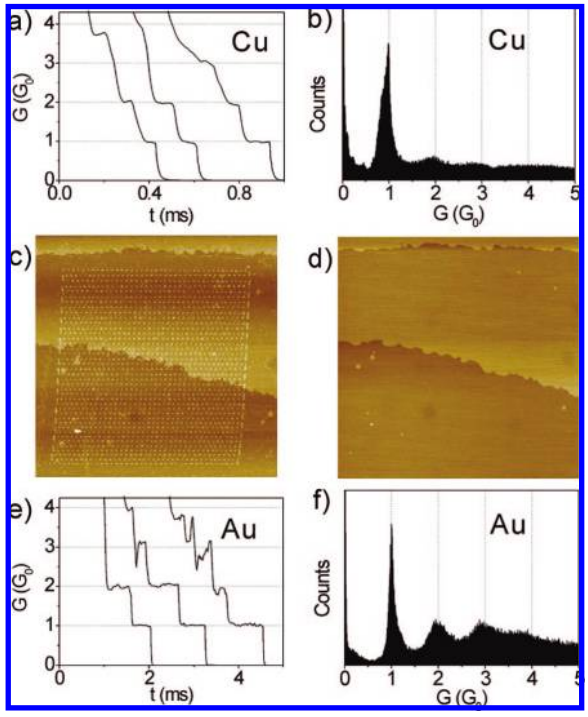

Figure 2. (a) Typical conductance traces and (b) the conductance histogram of Cu from 1600 traces. (c) STM image (800 × 800 nm^2) of 40 × 40 array of Cu clusters simultaneously generated upon contact breaking and (d) the same surface after dissolving the Cu clusters. (e, f) Au quantum conductance measured using the conventional STM-BJ after the dissolution of Cu clusters and the histogram constructed from 1000 traces without data selection. Bias (tip vs substrate) = −25 mV.

carried out in the aqueous solution of 1 mM $CuSO_4$ + 50 mM H_2SO_4. The Au tip was controlled at −23 mV vs Cu wire for Cu bulk deposition, while the Au(111) substrate was controlled at potentials slightly positive of the Nernst potential where Cu bulk deposition cannot proceed. Typical tip current and z-piezo voltage (U_z) measured from the STM system are shown in Figure 1e and f. A current as high as 73 μA was detected upon contact, which is equivalent to ∼40 G_0 ($G_0 = 2e^2/h$, where e is the electron charge and h is Plank's constant). Figure 2a gives typical conductance traces of Cu. The conductance has a clear stepwise feature in the last two plateaus at near multiples of 1 G_0 and drops sharply from the last plateau into the tunnelling current regime. The histogram constructed from 1600 traces without data selection is given by Figure 2b, and the most preferential conductance is found at ∼1 G_0 corresponding to the point-contact conductance of a fully open single channel.[6,27] Although peaks at multiples of 1 G_0 are rather weak, a small yet distinguishable peak can be found at 2 G_0. These characteristics are in agreement with those reported in the literature using various other approaches and in various environments.[1,8,18]

Several further steps were taken to prove the success of the present approach. First, along with the 1600 repetitive measurements fulfilled at designed positions in a 40 × 40 array, a corresponding array of Cu clusters is generated simultaneously as a side product, Figure 2c. The clusters are ∼6 nm at full width at half-maximum (fwhm) and 0.6 nm in height, verifying that the jump-to-contact occurred with Cu atoms transferring from the tip to the substrate. Next, these clusters can be removed completely at a sufficiently positive potential (e.g., 0.3 V), leaving a bare substrate surface, Figure 2d. Although surface alloying between Au(111) and the Cu cluster still cannot be completely excluded,[28] it is the conductance of Cu, not the alloy, that has been measured by the present approach. Otherwise, the preferential point-contact conductance on the

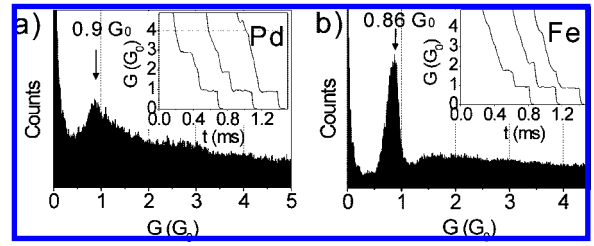

Figure 3. The conductance histograms of (a) Pd and (b) Fe. Insets of (a) and (b): typical conductance traces of Pd and Fe obtained in $BMIBF_4$ ionic liquid, respectively.

histogram would have been at least diminished in peak height as has been observed for Au−Pd and Au−Ag alloy nanocontacts.[29] Finally, an internal calibration of conductance was performed after the Cu conductance measurements. For this purpose, the potentials of both the tip and substrate were controlled at sufficiently positive potentials to recover the bare Au tip and surface, and hence the conductance was measured by the conventional STM-BJ with the tip crashing mechanism. The most preferential conductance of Au at 1 G_0 is determined from the conductance histogram (Figure 2e and f).

The above-proven approach is advantageous for conductance measurement of transition and magnetic metals, such as Pd and Fe for which the conductance has been found difficult to measure by other approaches, especially at room temperature. For Pd, by using the conventional STM-BJ technique, Murakoshi and co-workers obtained a point-contact conductance of 0.9 G_0 in solution, but only with the assistance of hydrogen evolution reaction (HER).[8] (also see Note S1) Our measurements of Pd conductance were performed in the aqueous solution of 1 mM $PdSO_4$ + 100 mM H_2SO_4 with the Au tip and Au(111) substrate potentials controlled at −23 mV and 2 mV vs Pd wire, respectively. In this case, a hydrogen evolution reaction (HER) is avoided and the complexity due to an absorbed hydrogen influence is removed. As shown in the inset of Figure 3a, well-defined final plateaus at near 1 G_0, corresponding to single-atom contacts, are distinguished despite the complicated stepwise decrease of conductance at high values of some traces. The conductance histogram constructed from 1600 of such traces gives a statistic preference of conductance at near 1 G_0 (i.e., 0.9 G_0) as shown in Figure 3a. The appearance of the well-defined single peak reveals that stable point-contact configurations can be attained by STM-BJ without hydrogen assistance at room temperature.

For the conductance measurement of the active magnetic metal of Fe, we employed a 1-butyl-3-methylimidazolium tetrafluoroborate ($BMIBF_4$) room temperature ionic liquid as the solvent[30,31] with ∼50 mM of dissolved $FeCl_3$. The Au tip and substrate were controlled at −775 and −750 mV vs Ag/AgCl,[25] respectively. As shown in the inset of Figure 3b, the conductance drops with a clear stepwise feature at the last two plateaus, which yields a sharp peak, though relatively small, of the point-contact conductance at near 0.86 G_0 on the conductance histogram as shown in Figure 3b.

Both the point-contact conductance of Pd (0.9 G_0) and Fe (0.86 G_0) measured in the present work are much smaller than the theoretical prediction for metals with five conduction channels as well as some experimental data reported in low temperature UHV.[7,8] It cannot be distinguished whether all channels are active but with low transmission probability or only some of the channels contribute significantly. It may be necessary to point out that various factors in the electrochemical environment such as adsorption of solvent, molecules, and ions at the atomic constriction may reduce the conductance of the atomic-size nanowires because of increased scattering of electron transport.[32,33] In addition, the application of

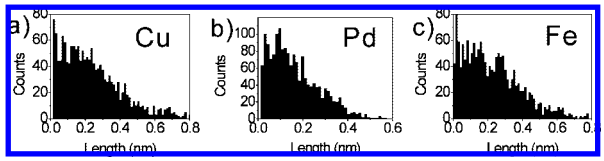

Figure 4. Length distributions of the last plateau of (a) Cu, (b) Pd, and (c) Fe.

the electrochemical potential may break the charge neutrality at the nanoconstriction, which would cause the shift of the Fermi energy level off the resonant state and thus reduction of the conductance.[2,34]

The apparent M_1-M_2 heterojunctions in the present approach might provoke a question on whether potential barriers are created at these junctions, which would otherwise affect the conductance value because of the bias voltage shift. However, the barriers, if any, could be canceled out considering the symmetric configurations of the two heterojunctions at the tip and the substrate. We also took Fe as an example and performed similar measurements with other combinations of the tip and substrate, namely a Pt−Ir tip and Au(111) and Au tip and Pt(111). Interestingly, the same values of Fe point-contact conductance were obtained within experimental error regardless of the unsymmeteric configuration of the heterojunctions (Figure S2).

We also tested the possible influence of the cluster size. Taking Cu as an example, larger clusters (∼1 nm in height and 5.5 nm in fwhm) were generated under the higher external voltage pulse, and the result remains the same; i.e., the point-contact conductance of Cu is near 1 G_0 (Figure S3). This leads to the conclusion that the numbers of atom contained in the clusters are sufficiently large to include all possible configurations for accurate conductance measurements and the measured conductance reflects the intrinsic nature of the metal in the environment employed.

Finally, it is noteworthy that the retraction of the piezo is fulfilled with a linear decrease of the voltage at a speed of ∼1600 nm·s^{-1}, which is much faster than that used in the conventional STM-BJ (10−100 nm·s^{-1}). A direct benefit from this fast tip withdrawal speed is the reduced noise of the current trace because of suppression of the mechanical drift of the STM system. This does not, however, degrade severely the nanomechanical behaviors of atomic-size wires as can be judged from the well-defined final plateaus on the conductance traces as well as the length histograms. For all three metals, Cu, Pd, and Fe, a common feature of the conductance traces is that the final plateaus hold longer against stretching (Figure 4). For Pd, the length histogram shows a statistical preferential peak with the tail at the long-distance side extending up to 0.5 nm (Note S2).

In conclusion, we have presented an electrochemical strategy for the STM-BJ technique, which extends the capability to establish stable metallic atomic-size nanowires. Together with the employment of room temperature ionic liquids, this strategy has been proven by the successful conductance measurements of not only Cu but also Pd and Fe. It promotes further investigations on quantized transport through atomic-size nanowires, especially the magnetic nanowires whose electron transport may be modified by spin polarization at the atomic contact. In addition, it may open up an opportunity to study soft metals such as Cd, or even liquid metals such as Hg. Equally important is that it provides the feasibility to form metal-molecule-metal junctions with a variety of choices of metals in the junction, which is highly desirable for a systematic investigation of the role of molecule-metal interaction in single molecule conductance. These works are currently in progress in the authors' laboratory.

Acknowledgment. The authors gratefully thank Prof. D. M. Kolb for providing knowledge to interface the external electronic control with the STM and Prof. N. J. Tao for valuable discussions. This work was supported by NSFC (No. 20433040, 20273056, 90406024) and Key Scientific Project of Fujian Province, China (2005HZ01-3).

Supporting Information Available: Experimental details, supplemental discussion, STM images of metal clusters and their dissolution, conductance of Cu with larger clusters, and Fe histograms with various tip and substrate combination. This material is available free of charge via the Internet at http://pubs.acs.org.

References

(1) Agraït, N.; Yeyati, A. L.; van Ruitenbeek, J. M. *Phys. Rep.* **2003**, *377*, 81–279.
(2) Shu, C.; Li, C. Z.; He, H. X.; Bogozi, A.; Bunch, J. S.; Tao, N. J. *Phys. Rev. Lett.* **2000**, *84*, 5196–5199.
(3) Kiguchi, M.; Murakoshi, K. *Appl. Phys. Lett.* **2006**, *88*, 253112.
(4) Ohnishi, H.; Kondo, Y.; Takayanagi, K. *Nature* **1998**, *395*, 780–783.
(5) Untiedt, C.; Caturla, M. J.; Calvo, M. R.; Palacios, J. J.; Segers, R. C.; van Ruitenbeek, J. M. *Phys. Rev. Lett.* **2007**, *98*, 206801.
(6) Scheer, E.; Agraït, N.; Cuevas, J. C.; Yeyati, A. L.; Ludoph, B.; Martin-Rodero, A.; Bollinger, G. R.; van Ruitenbeek, J. M.; Urbina, C. *Nature* **1998**, *394*, 154–157.
(7) Csonka, S.; Halbritter, A.; Mihaly, G.; Shklyarevskii, O. I.; Speller, S.; van Kempen, H. *Phys. Rev. Lett.* **2004**, *93*, 016802.
(8) Ludoph, B.; van Ruitenbeek, J. M. *Phys. Rev. B* **2000**, *61*, 2273–2285.
(9) Costa-Kramer, J. L. *Phys. Rev. B* **1997**, *55*, R4875−R4878.
(10) Chen, F.; Hihath, J.; Huang, Z. F.; Li, X. L.; Tao, N. J. *Annu. Rev. Phys. Chem.* **2007**, *58*, 535–564.
(11) Xiao, X. Y.; Nagahara, L. A.; Rawlett, A. M.; Tao, N. J. *J. Am. Chem. Soc.* **2005**, *127*, 9235–9240.
(12) van Zalinge, H.; Schiffrin, D. J.; Bates, A. D.; Starikov, E. B.; Wenzel, W.; Nichols, R. J. *Angew. Chem., Int. Ed.* **2006**, *45*, 5499–5502.
(13) Li, C.; Pobelov, I.; Wandlowski, T.; Bagrets, A.; Arnold, A.; Evers, F. *J. Am. Chem. Soc.* **2008**, *130*, 318–326.
(14) Zhou, X. S.; Chen, Z. B.; Liu, S. H.; Jin, S.; Liu, L.; Zhang, H. M.; Xie, Z. X.; Jiang, Y. B.; Mao, B. W. *J. Phys. Chem. C* **2008**, *112*, 3935–3940.
(15) Venkataraman, L.; Klare, J. E.; Nuckolls, C.; Hybertsen, M. S.; Steigerwald, M. L. *Nature* **2006**, *442*, 904–907.
(16) Park, J.; Pasupathy, A. N.; Goldsmith, J. I.; Chang, C.; Yaish, Y.; Petta, J. R.; Rinkoski, M.; Sethna, J. P.; Abruna, H. D.; McEuen, P. L.; Ralph, D. C. *Nature* **2002**, *417*, 722–725.
(17) Xu, B. Q. *Small* **2007**, *3*, 2061–2065.
(18) Li, C. Z.; Tao, N. J. *Appl. Phys. Lett.* **1998**, *72*, 894–896.
(19) Li, C. Z.; Bogozi, A.; Huang, W.; Tao, N. J. *Nanotechnology* **1999**, *10*, 221–223.
(20) Li, J. Z.; Kanzaki, T.; Murakoshi, K.; Nakato, Y. *Appl. Phys. Lett.* **2002**, *81*, 123–125.
(21) Miura, S.; Kiguchi, M.; Murakoshi, K. *Surf. Sci.* **2007**, *601*, 287–291.
(22) Kolb, D. M.; Ullmann, R.; Will, T. *Science* **1997**, *275*, 1097–1099.
(23) Engelmann, G. E.; Ziegler, J. C.; Kolb, D. M. *J. Electrochem. Soc.* **1998**, *145*, L33−L35.
(24) Wang, J. G.; Tang, J.; Fu, Y. C.; Wei, Y. M.; Chen, Z. B.; Mao, B. W. *Electrochem. Commun.* **2007**, *9*, 633–638.
(25) Wei, Y. M.; Zhou, X. S.; Wang, J. G.; Tang, J.; Mao, B. W.; Kolb, D. M. *Small* **2008**, *4*, 1355–1358.
(26) Kolb, D. M.; Engelmann, G. E.; Ziegler, J. C. *Angew. Chem., Int. Ed.* **2000**, *39*, 1123–1125.
(27) Bakker, D. J.; Noat, Y.; Yanson, A. I.; van Ruitenbeek, J. M. *Phys. Rev. B* **2002**, *65*, 235416.
(28) Del Popolo, M. G.; Leiva, E. P. M.; Mariscal, M.; Schmickler, W. *Surf. Sci.* **2005**, *597*, 133–155.
(29) Enomoto, A.; Kurokawa, S.; Sakai, A. *Phys. Rev. B* **2002**, *65*, 125410.
(30) Lin, L. G.; Wang, Y.; Yan, J. W.; Yuan, Y. Z.; Xiang, J.; Mao, B. W. *Electrochem. Commun.* **2003**, *5*, 995–999.
(31) Fu, Y. C.; Yan, J. W.; Wang, Y.; Tian, J. H.; Zhang, H. M.; Xie, Z. X.; Mao, B. W. *J. Phys. Chem. C* **2007**, *111*, 10467–10477.
(32) Xu, B. Q.; He, H. X.; Tao, N. J. *J. Am. Chem. Soc.* **2002**, *124*, 13568–13575.
(33) Bogozi, A.; Lam, O.; He, H.; Li, C.; Tao, N. J.; Nagahara, L. A.; Amlani, I.; Tsui, R. *J. Am. Chem. Soc.* **2001**, *123*, 4585–4590.
(34) Todorov, T. N.; Briggs, G. A. D.; Sutton, A. P. *J. Phys.: Condens. Matter* **1993**, *5*, 2389–2406.

JA8055276